A 350-Year Reconstruction of the Response of South Cascade Glacier to Interannual and Interdecadal Climatic Variability

Kailey Marcinkowski,[1,2] University of Washington, School of Environmental and Forest Sciences, Fire and Mountain Ecology Laboratory, Box 352100, Seattle, Washington 98195

and

David L. Peterson, U.S. Forest Service, Pacific Northwest Research Station, 400 N. 34th St., Suite 201, Seattle, Washington 98103

A 350-year Reconstruction of the Response of South Cascade Glacier to Interannual and Interdecadal Climatic Variability

Abstract

Mountain hemlock growth chronologies were used to reconstruct the mass balance of South Cascade Glacier, an alpine glacier in the North Cascade Range of Washington State. The net balance reconstruction spans 350 years, from 1659 to 2009. Summer and winter balances were reconstructed for 1346–2009 and 1615–2009, respectively. Relationships between mass balance and winter precipitation, temperature, the Pacific Decadal Oscillation index, and the El Niño Southern Oscillation index indicate that these influence glacier balance at various temporal scales. Above-average net, summer, and winter mass balance occurred mainly in 1690–1710, 1810–1820, 1845–1860, 1865–1890, and 1975–1990, and below-average balance periods include 1680–1690, 1790–1810, 1820–1840, and 1930–1960. Above- and below-average reconstructed mass balances at South Cascade Glacier were concurrent with similar periods from other glacier balance reconstructions in the Pacific Northwest region of North America. Agreement among these records suggests that changes in South Cascade Glacier mass balance are good indicators of regional balance fluctuations, and glaciers in the Pacific Northwest are responding similarly to regional external forcings. The current rate of decline, from 2000 to 2009, in the reconstructed balance record has been faster than any decline in a century. This decreasing trend is projected to continue with increasing temperatures, and will likely affect glacier-influenced water resources in the Pacific Northwest.

Keywords: dendrochronology, climate, glacier mass balance, North Cascades, South Cascade Glacier

Introduction

Since the 1980s, the majority of alpine glaciers in the Pacific Northwest (PNW) region of North America (British Columbia, Washington, and Oregon) have been receding rapidly (Hodge et al. 1998, Meier et al. 2003, Koch et al. 2009, Moore et al. 2009, Malcomb and Wiles 2013). This rapid retreat is frequently attributed to a shift in atmosphere and ocean circulations in the mid-1970s resulting in increased temperatures (McCabe and Fountain 1995, McCabe et al. 2000, Moore and Demuth 2001, Rasmussen and Conway 2004). The response of the terminus to climate is delayed because of complex ice dynamics, so changes in glacier volume are typically assessed using mass balance measurements that reflect an immediate response to climate (Walters and Meier 1989).

Weather patterns in the PNW affect glacier mass balance on different time scales through atmospheric circulation anomalies (McCabe and Fountain 1995, McCabe et al. 2000, Meier et al. 2003, Rasmussen and Conway 2004), sea surface temperatures and pressures (Hodge et al. 1998, Bitz and Battisti 1999, Moore and Demuth 2001, Pederson et al. 2004, Watson et al. 2006, Pelto 2008), and annual or seasonal climatic variables (Burbank 1982, Rasmussen 2009, Wood et al. 2011). Glacier mass balance also responds to storm tracks moving through the PNW (McCabe and Fountain 1995, Hodge et al. 1998, Bitz and Battisti 1999, McCabe et al. 2000). Although it is generally assumed that summer temperature and winter precipitation drive mass balance fluctuations, the relationship between climate and mass balance is complicated by glacial ice dynamics (Burbank 1982, Bitz and Battisti 1999). In maritime

climates on the west side of the Cascade Range, winter precipitation, and therefore winter mass balance, dominates net balance (Bitz and Battisti 1999, Dyurgerov and Meier 1999).

The El Niño Southern Oscillation (ENSO) is correlated with PNW storminess and weather. El Niño winters are associated with warm, dry air flowing into the Northwest, and La Niña winters are associated with more storms and cooler temperatures. Differences in ENSO phases are correlated with changes in glacier mass balance (Hodge et al. 1998, Bitz and Battisti 1999, Moore and Demuth 2001, Larocque and Smith 2005, Watson et al. 2006, Pelto 2008, Wood et al. 2011). The Pacific Decadal Oscillation (PDO) is also correlated with PNW weather but at 20–40 year scales (Mantua 1997). The warm phase PDO is similar to El Niño, because it is associated with warmer, drier weather in the PNW, and the cool phase PDO is similar to La Niña, because it is associated with cooler, wetter weather (especially in winter). Several studies have documented correlations between PDO index and glacier mass balance (Hodge et al. 1998, Bitz and Battisti 1999, Moore and Demuth 2001, Lewis and Smith 2004, Pederson et al. 2004, Larocque and Smith 2005, Watson et al. 2006, Pelto 2008, Wood et al. 2011, Malcomb and Wiles 2013).

Tree-ring chronologies can be used as proxies for glacial mass balance because similar climatic variables influence glaciers and tree growth (Lewis and Smith 2004, Watson and Luckman 2004, Larocque and Smith 2005, Wood et al. 2011, Wood and Smith 2012, Malcomb and Wiles 2013). Mountain hemlock (*Tsuga mertensiana*) is a suitable proxy for glacial mass balance because it grows at high elevations and experiences similar climate as glaciers. In the PNW, mountain hemlock growth at high elevations (> 1500 m) is sensitive to winter precipitation (snowpack), which affects the length of growing season (Peterson and Peterson 2001), and growth is therefore also correlated with winter PDO index (Gedalof and Smith 2001, Peterson and Peterson 2001). Favorable growth for mountain hemlock is associated with low snowpack and a long growing season, and unfavorable growth is associated with high snowpack and a short growing season.

Glacier mass balance is generally inversely related to mountain hemlock radial growth, and because mountain hemlock can live for several hundred years, mass balance based on tree-ring chronologies can be reconstructed for centuries prior to the observational record. In the PNW, Lewis and Smith (2004) used mountain hemlock chronologies to reconstruct mass balance of two glaciers on Vancouver Island, British Columbia (Canada). Watson and Luckman (2004) reconstructed mass balance at Peyto Glacier, British Columbia, from regional precipitation and temperature reconstructions using various tree species as proxies. Larocque and Smith (2005) examined correlations for mass balance of several glaciers and radial growth of several tree species to reconstruct a regional mass balance record for the PNW, including winter balance for South Cascade Glacier (SCG) (1835–1999). Wood et al. (2011) reconstructed mass balance of Place Glacier, British Columbia, from tree-ring width and maximum ring density chronologies of Engelmann spruce (*Picea engelmannii*). Similarly, Wood and Smith (2012) used tree-ring width, maximum ring density, and maximum cell wall thickness chronologies from three high-elevation tree species to reconstruct the mass balance of glaciers in the Columbia Mountains of British Columbia. Malcomb and Wiles (2013) reconstructed the annual mass balance of six glaciers in the PNW including SCG (1580–1992) and examined correlations between the reconstructed mass balances and climatic variables.

Examining SCG mass balance changes has broad implications for other glaciers with similar climatic regimes and topographic features. Variation in year-to-year net balance at SCG is correlated with that of adjacent glaciers (Pelto 2008, Fountain et al. 2009), and similarly to trends at SCG, the majority of PNW glaciers have been receding (Hodge et al. 1998, Granshaw and Fountain 2006, Pelto 2006, Koch et al. 2009). Because of this connection, regional glacier mass balance can be expected to follow trends at SCG.

South Cascade Glacier, in the Cascade Range in Washington State, is a prime location to reconstruct glacial balance because of its history of mass

balance measurements. In this study, we expand on Larocque and Smith (2005) and Malcomb and Wiles (2013) by (1) focusing solely on SCG, (2) sampling sites closer to SCG, and (3) including recent years in the tree-ring chronologies and mass balance record (ending 2009 vs. 1999 and 1992). Specifically, we reconstructed SCG net, summer, and winter mass balance from mountain hemlock growth chronologies surrounding the glacier. Closer proximity of sampling sites and a longer calibration interval are expected to produce a more robust analysis of SCG mass balance. Other glacier mass balance reconstructions and moraine dates from the PNW were compared to the SCG reconstruction to determine if broad synchrony in past balance exists. Rates of change during periods of above- and below-average reconstructed mass balance were calculated, providing a context for projecting the potential effects of future temperature increase on mass balance.

Methods

Study Site

South Cascade Glacier is located at 48.355278, -121.0575 within the Cascade Range in Washington State. The glacier is in a north-northwest facing valley with an altitude range of 1600–2100 meters (Bidlake et al. 2010). Meltwater from the glacier flows into South Cascade Lake, the headwaters of the South Fork of the Cascade River. The Cascade River connects with the Skagit River and empties into Puget Sound.

South Cascade Glacier has one of the longest, most complete records of mass balance measurements in North America. The U.S. Geological Sur-

vey (USGS) considers SCG a benchmark glacier, a regional representation that is measured annually for mass balance and other variables (Fountain et al. 2009), with measurements beginning in 1959. Annual fluctuations in net mass balance at SCG are highly correlated with those of surrounding glaciers and can be interpreted as representative of year-to-year balance variations (Pelto 2008, Fountain et al. 2009). Since the USGS began monitoring, SCG has retreated 0.7 km from its 1958 terminus position, and the area has shrunk from 2.71 km^2 in 1958 to 1.73 km^2 in 2007 (Bidlake et al. 2010). Net, winter, and summer mass balance values for 1959–2009 were used in this study (Bidlake et al. 2010 [1959–2007], William R. Bidlake, U.S. Geological Survey, personal communication [2008–2009]).

Models based on temperature and precipitation observations were used by Tangborn (1980) to estimate SCG net balance for 1884–1974, and by Rasmussen (2009) to reconstruct SCG balance for 1935–1958 and adjust values for 1959–2006. Combined, these studies found mostly below-average mass balance from 1900 to 1940 and above-average balance from 1950 to 1980. Other studies involving SCG found mass balance to be influenced by atmospheric and ocean circulation indices (McCabe and Fountain 1995, Hodge et al. 1998, Burbank and Battisti 1999, McCabe et al. 2000, Larocque and Smith 2005, Malcolmb and Wiles 2013).

Chronology Construction

Four high-elevation forests surrounding SCG in the North Cascade Range were sampled in summer 2011 (Table 1). All sites are within 75 km of SCG

TABLE 1. A summary of site and tree characteristics. Mean diameter at breast height (DBH) represents the average diameter and standard deviation (SD) for trees at each site.

Site	Hidden Lake (HL)	South Cascade (SC)	Bagley Lakes (BL)	Minotaur Lake (ML)
Mean elevation (m)	1769	1613	1297	1703
Longitude	-121.208797	-121.078867	-121.685031	-121.035894
Latitude	48.5037562	48.3736037	48.8606919	47.8443795
Mean DBH (SD) (cm)	51.7 (5.7)	76.8 (12.6)	68.6 (8.1)	51.3 (8.6)
Year range	1346–2010	1392–2010	1659–2010	1615–2010
Median age (yr)	371	349	298	296
Mean age (yr)	385	367	302	293

(Figure 1). Twenty mountain hemlock trees were sampled at each site, with preference given to the largest, dominant, or co-dominant trees without signs of disturbances (i.e. fire, insects, wind). Trees
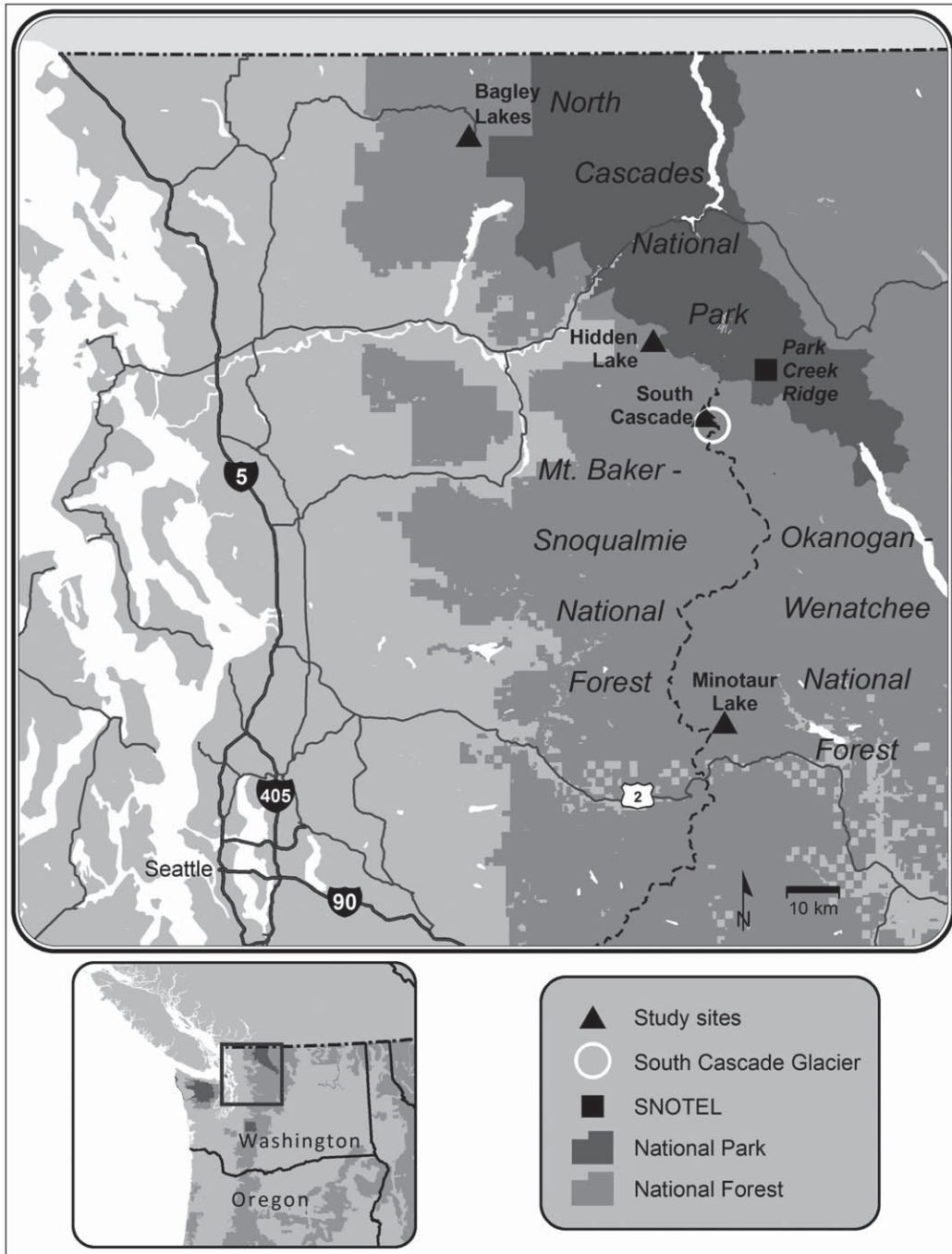
Figure 1. Map of study sites. Triangles represent sampling locations, the white circle represents the location of South Cascade Glacier, and the square represents the SNOTEL site used in the climate-growth correlations. Shaded light gray areas indicate National Forest lands, and shaded dark gray areas indicate National Parks.

were sampled at breast height with an increment borer at the cross-slope position of the bole in order to reduce the likelihood of encountering compression wood.

The cores were air dried and glued to mounting boards. Cores were sanded with progressively finer grades of sandpaper until the ring pattern was clearly visible and annual ring boundaries were identifiable. The tree rings were crossdated using standard dendrochronology procedures (Stokes and Smiley 1968). For each tree, the most intact or longest core was chosen, and the ring widths were measured and recorded to the nearest 0.001 mm. Crossdating was verified, and any missing or false rings were corrected, using the program COFECHA (Holmes 1983).

Tree-ring series were detrended with ARSTAN (Cook and Holmes 1996). Detrending removes trends caused by tree age and growth characteristics. When trees first establish, rings are wide because the circumference of the tree is small, but as trees age the widths of the rings decrease to accommodate increasing circumference. Several detrending curves were explored before a cubic spline with a 50% cutoff of 150 years was chosen (Table 2). Upon examination of descriptive curve statistics (Fritts 1976), it was determined that splines of different smoothness had similar results.

The stiff cubic spline was selected because the majority of the samples did not display juvenile growth in the innermost rings or a negative exponential decline afterward. Most trees were older than 250 years and rotten towards the middle, so often the pith was not recovered. This led to most series exhibiting the radial growth trends of mature trees. For the few trees that did seem to have an age-related decline, the stiff spline matched the curve as well as a negative exponential fit.

A unitless index was calculated for each detrended series by dividing the measured observations by the fitted curve values for easier comparisons and averaging between individual series. The indexed series were prewhitened with an autoregressive (AR) model to remove autocorrelation effects from the biological persistence of individual trees. AR modeling generates a residual chronology that is uncorrelated with past or future values. The residual series and the standard, non-prewhitened series were then averaged into separate site chronologies using a bi-weight robust mean. Both residual and standard chronologies were prepared to examine which representation of growth was a better fit for reconstructing SCG mass balance. Cutoff dates were not chosen for the site chronologies; instead, the entire length of the chronologies was utilized. Because of this, the further back in time the chronologies reach, the sample depth decreases and the variance may be artificially inflated. The calculation of indices, AR models, and site chronologies was done using ARSTAN (Cook and Holmes 1996).

Principal components analyses (PCA) were conducted on the four residual site chronologies and the four standard chronologies separately to identify the common variance among the sites. Because the sites surrounded SCG, we wanted

TABLE 2. Summary of chronology statistics. Series mean first-order autocorrelation and mean interseries correlation values are prior to autoregressive modeling and are the same for both standard and residual chronologies. Mean sensitivity values are calculated after autoregressive modeling and apply to the residual chronologies.

Site	Hidden Lake	South Cascade	Bagley Lakes	Minotaur Lake
n	17	17	19	18
Series mean first-order autocorrelation	0.480	0.371	0.386	0.549
Mean interseries correlation (r_{avg})	0.294	0.318	0.299	0.307
Mean sensitivity	0.231	0.186	0.191	0.191
Autoregressive Order	4	2	2	2
Autoregressive R^2	0.24	0.15	0.17	0.33

to find a commonality between them that might better represent changes in SCG mass balance and add strength to our results. A common interval of 1659–2009 was used. The end point for this interval is the last year of mass balance measurements currently available, and the start date is the earliest year of the shortest growth chronology among the four sites.

Climate Data

Divisional climatic data were obtained from the National Climatic Data Center for 1896–2009 (NCDC 1994, after Karl et al. 1986). Divisional data are a compilation of individual stations within regions thought to have similar climate. Because the divisional data are derived from multiple stations, they better represent regional climate and have a longer record than any one station. Monthly total precipitation and average temperature were used from two climatic divisions; the Hidden Lake (HL), South Cascade (SC), and Bagley Lakes (BL) sites, and SCG all fell within the boundaries of the western Washington Cascades, and the Minotaur Lake (ML) site was located just inside the eastern Washington Cascades divisional border. The ML site is within the eastern Cascades boundary as defined by the National Climatic Data Center; however, we believe that the ML site does not have the typical eastern Cascades climate of lower snowpack and higher temperatures compared with the western Cascades. The Park Creek Ridge SNOTEL site was used for April 1 snow water equivalent (SWE) record for 1936–2009, and the Park Creek Ridge snow course record was used for April 1 snow depth for 1936–1992. Park Creek Ridge was chosen because it is the closest observation site to SCG.

The Pacific North American index (PNA) was obtained from the National Weather Service Climate Prediction Center for 1950–2009 (NOAA 2012); the Pacific Decadal Oscillation index (PDO) was obtained from the Joint Institute for the Study of the Atmosphere and Ocean climate data archives for 1901–2009 (University of Washington 2014); and the Niño Region 3.4 Index (ENSO) was retrieved from the National Center for Atmospheric Research for 1872–2007 (NCAR 2008). These indices were chosen to explore which ocean-atmospheric circulation modes affect tree growth and SCG mass balance, because results on the importance of different circulation modes varied in other studies (Hodge et al. 1998, Bitz and Battisti 1999, Moore and Demuth 2001, Lewis and Smith 2004, Pederson et al. 2004, Larocque and Smith 2005, Watson et al. 2006, Pelto 2008, Wood et al. 2011, Malcomb and Wiles 2013).

The residual and standard chronologies from the sites were compared to the current and previous water year (October–September) divisional climatic data and ocean indices by month using Pearson product-moment correlations. Net, summer, and winter measured mass balance values were also compared to current and previous year climatic and circulation variables using product-moment correlations. Correlations were calculated for April 1 SWE, April 1 snowpack depth, total winter (October–March) precipitation, and average winter and spring (March–May) PDO and ENSO indices with the chronologies and observed mass balance data.

Mass Balance Reconstruction

Pearson product-moment correlations were calculated between each of the four residual and standard chronologies and the first principal components (PC1) derived from the PCAs, and summer, winter, and net mass balance measurements. This was done to determine if there was a statistically significant ($P < 0.05$) relationship between the site chronologies and the balance measurements. Simple linear regression analyses were conducted for each of the chronologies and PC1s with net, summer, and winter mass balance, where mass balance was the dependent variable and site-specific growth indices the independent variable. Coefficients of determination (R^2) were calculated for each regression model, and residuals were examined for departures from normality and autocorrelation. When a significant relationship ($P < 0.05$) between tree growth and mass balance existed, the growth indices were used in the regression equation to reconstruct mass balance. R^2 was used as the criterion for choosing which regression model was used to represent net, winter,

and summer balance, and the chosen regression models were examined for autocorrelation with the Durbin-Watson (D-W) test and skill in prediction with the Reduction of Error (RE) statistic. All calculations and graphs in this study were created using R (Version 0.94.110 [software]. R Core Development Team 2010).

Results

Climate Correlations

Pearson product-moment correlations between climatic variables and tree growth were conducted for both the standard and residual chronologies. Because the standard chronologies were not prewhitened, the sample size must be adjusted to account for autocorrelation. In doing this, the power of the analysis was reduced and few relationships were found to be significant. The residual chronologies, having already accounted for autocorrelation, produced many significant results and were considered better for use in the correlation analysis.

Correlations between the residual growth chronologies and monthly climatic variables were explored for the four sampling sites (Table 3). Previous-year July and August temperatures were negatively correlated with growth, and December temperature was positively correlated with current year growth. All sites had similar patterns for

TABLE 3. Sign (+, -) of significant ($P < 0.05$) correlation coefficients between residual growth chronologies and measured glacier mass balance with monthly temperature (T), precipitation (P), the Pacific Decadal Oscillation index (PDO), and the El Niño Southern Oscillation index (E). Sample size (n) for growth correlations is T = 115, P = 115, PDO = 109, E = 136, and mass balance sample size is T = 51, P = 51, PDO = 51, E = 49.

Previous Growth Year	Hidden Lake				Bagley Lakes				Minotaur Lake				South Cascade				Net balance				Summer balance				Winter balance			
	T	P	PDO	E	T	P	PDO	E	T	P	PDO	E	T	P	PDO	E	T	P	PDO	E	T	P	PDO	E	T	P	PDO	E
O		+	-		+		-	-							-	-												
N			-				-	-			-				-	-												
D			-				-	-			-																	
J	-				-		-	-					-		-													
F		-					-	-								-						+						
M						+							-	+	-	-												
A								-																				
M											-									-								
J				+																-			-					-
J				+	-	+		-				-	-							-			-				-	-
A	-			+	-								-						-	-			-				-	-
S				+												+			-	-			-				-	-

Current Growth Year	Hidden Lake				Bagley Lakes				Minotaur Lake				South Cascade				Net balance				Summer balance				Winter balance			
	T	P	PDO	E	T	P	PDO	E	T	P	PDO	E	T	P	PDO	E	T	P	PDO	E	T	P	PDO	E	T	P	PDO	E
O				+								+				+	-	+	-	-				-	-	+	-	-
N	+			+					+	+						+	+		-	-				-		+	-	-
D	+		+	+					+				+		+	+	+		-	-				-		+	-	-
J			+	+					+		+	+		+	+	+	+		-	-				-		+	-	-
F		-	+	+		-			-		+	+	-		+	+	+		-	-				-		+	-	-
M			+		+	-			+		+	+			+		-		-	-				-	-	+	-	-
A		-	+	+			+	+				+	-		+		-		-	-				-	-		-	-
M			+					+					+				-		-	-	-		-				-	
J				+				+	+				+				-		-		-	+					-	
J	+	-				-											-				-						-	
A									-				-				-				-	+						
S																					-							

TABLE 4. Sign (+, -) of significant ($P < 0.05$) correlation coefficients between residual growth chronologies and measured glacier mass balance and climatic variables. Winter Pacific Decadal Oscillation (PDO), El Niño Southern Oscillation (ENSO), and precipitation are averaged for October-March, and spring values are averaged for March-May. Sample size (n) is listed for both mass balance and growth correlations.

Climate variable	Mass balance				Growth chronology				
	n	Net	Summer	Winter	n	Hidden Lake	South Cascade	Bagley Lakes	Minotaur Lake
Winter PDO	51	-		-	109	+			+
Spring PDO	51	-		-	109	+			+
Winter ENSO	49	-	-	-	136	+	+		
Spring ENSO	49	-	-	-	136	+	+	+	
April 1 snowpack depth	34	+		+	56		-	-	-
April 1 snow-water-equivalent	51	+	+	+	74	-	-	-	-
Winter precipitation	51	+	+	+	115	-	-	-	

correlations with temperature and growth, where correlations switched from negative to positive during previous year summer months. Correlations were negative between February precipitation and growth at all sites, and total winter precipitation and growth were negatively correlated for three sites. Both April 1 snowpack depth and SWE were negatively correlated with growth, indicating that radial growth at the sampling sites is sensitive to precipitation during winter months (Table 4).

Mass balance measurements were correlated with monthly climatic variables (Table 3). Temperatures in October, March, and April were correlated negatively with winter and net balance, and May–June temperatures were negatively correlated with net and summer balance. October–February precipitation had a positive relationship with winter and net balance, and total winter precipitation correlated positively to all balances. April 1 SWE was positively correlated with all balances, and April 1 snowpack had positive correlations with net and winter balance. Correlations with PDO, precipitation, snowpack, and SWE indicate that net, winter, and sometimes summer balances are positively influenced by winter-month precipitations (Table 4).

Correlations between circulation indices and tree growth were also examined by month (Table 3). PNA did not have significantly strong correlations or agreement among the sites. December, January, and April PDO were positively correlated to tree growth. Previous-year November and December

PDO were negatively correlated at all sites, with October and February negatively correlated with three sites. However, average winter PDO was significantly correlated to growth only at HL and ML. Tree growth and January–April ENSO values had a positive relationship. Winter ENSO was significant for growth only at SC and HL, but spring ENSO had significant correlations for SC, HL, and BL. Correlations between current year growth, PDO, and ENSO indicate that radial growth is higher during warm phases of these cycles and lower during cool phases. Patterns in PDO and ENSO correlations were consistent. Correlations switched from negative to positive during late spring or summer of the previous growth year, and winter-month PDO and ENSO values had the most influence on growth.

The same circulation variables were examined for correlations with net, winter, and summer mass balance (Table 3). January, March, and April PNA were negatively correlated with net and winter balance, and July PNA was negatively correlated with summer and net balance. Previous year August–September and current year October–June PDO values were negatively correlated with winter and net balances. Average winter and spring PDO indices had significant negative relationships with winter and net balance. Summer balance had no significant correlations with PDO. All balances had significant negative correlations with previous year June–September and current year October–April ENSO. Winter and spring

ENSO had significant negative correlations with all balances. The correlations with PNA, PDO, and ENSO suggest that these circulation indices influence mass balance similarly.

South Cascade Glacier Mass Balance Reconstruction

The PCAs produced four components for both the standard and residual chronologies. The first principal component (PC1) accounted for 67% of the variance among the residual chronologies. PC2 explained an additional 14% of the variance. PC1 explained 66% of the variance among the standard chronologies. Because both PC1s explained most of the variance in the chronologies, they were assumed to be sufficient representations of the common growth variability at all sites.

Because of autocorrelation in the standard chronologies, sample size was reduced and most correlations between growth and mass balance were not significant. Net balance correlations with the standard chronologies were significant only for ML and PC1, summer balance had a significant relationship with HL and PC1, and winter balance was correlated with ML and BL. Correlations between all residual site chronologies and PC1 and net balance were significant ($P < 0.05$). All residual chronologies except SC had significant

relationships with winter balance, and PC1, HL, and SC were correlated with summer balance.

The standard and residual chronologies, including the PC1s, were used separately in simple linear regressions with net, winter, and summer mass balance to compare sensitivity of the regression analysis to chronology approach. The regression produced similar R^2 results and prediction equations, but most residual chronologies produced higher R^2 values. Because the analysis did not seem to be sensitive to the chronology approach, the residual chronologies were chosen to continue the analysis because of higher correlation coefficients with mass balance, higher R^2 values, and absence of autocorrelation in the series (Table 5).

Examination of model statistics and residuals revealed that all five regressions using the residual chronologies were significant ($P < 0.05$), and a simple linear regression was sufficient and could be used to reconstruct net balance. Although all reconstructions had comparable results, PC1 was chosen to reconstruct net balance, because it displayed a common growth pattern among the four sites. PC1 did not have the highest R^2 value, but it was thought to include both winter and summer balance signals. Winter balance had the highest correlation and R^2 value with the ML chronology and was reconstructed from its growth

TABLE 5. Summary of regression statistics for each residual site chronology and glacier mass balance. Correlations (r) are significant ($P < 0.05$) at the threshold value of $r = 0.28$ ($n = 51$). All R^2 listed are significant ($P < 0.05$). Mass balance is the dependent variable (y), and the residual chronologies are the independent variable (x). Regression models have normal, independent residuals, and the chosen models (indicated in **bold**) were examined for autocorrelation with the Durbin Watson (D-W) test (reported values are nonsignficant, indicating that autocorrelation is not present) and the Reduction of Error (RE) statistic (positive values indicate that the regression equation has skill in prediction).

	Net balance			Summer balance			Winter balance			Validation statistics	
Site	r	R^2	Equation	r	R^2	Equation	r	R^2	Equation	D-W	RE
Hidden Lake	-0.47	0.22	$y = 2.497 - 3.157x$	-0.42	0.18	**$y = -1.494 - 1.878x$**	-0.29	0.08	$y = 3.990 - 1.279x$	1.640	0.179
South Cascade	-0.33	0.11	$y = 1.326 - 1.966x$	-0.32	0.10	$y = -2.091 - 1.271x$	-0.18	NS	–		
Bagley Lakes	-0.31	0.09	$y = 1.352 - 1.964x$	-0.13	NS	–	-0.33	0.11	$y = 4.134 - 1.412x$		
Minotaur Lake	-0.37	0.14	$y = 1.826 - 2.455x$	-0.15	NS	–	-0.41	0.17	**$y = 4.519 - 1.810x$**	1.693	0.171
PC1	0.43	0.18	**$y = -0.626 + 1.616x$**	0.30	0.09	$y = -3.345 + 0.740x$	0.35	0.13	$y = 2.720 + 0.875x$	1.703	0.184

index. Summer balance was reconstructed from the HL chronology, which had the highest correlation and R^2 value.

Figure 2 shows the reconstructed mass balance values plotted with the observed balance. Comparing the cumulative net mass balance of the
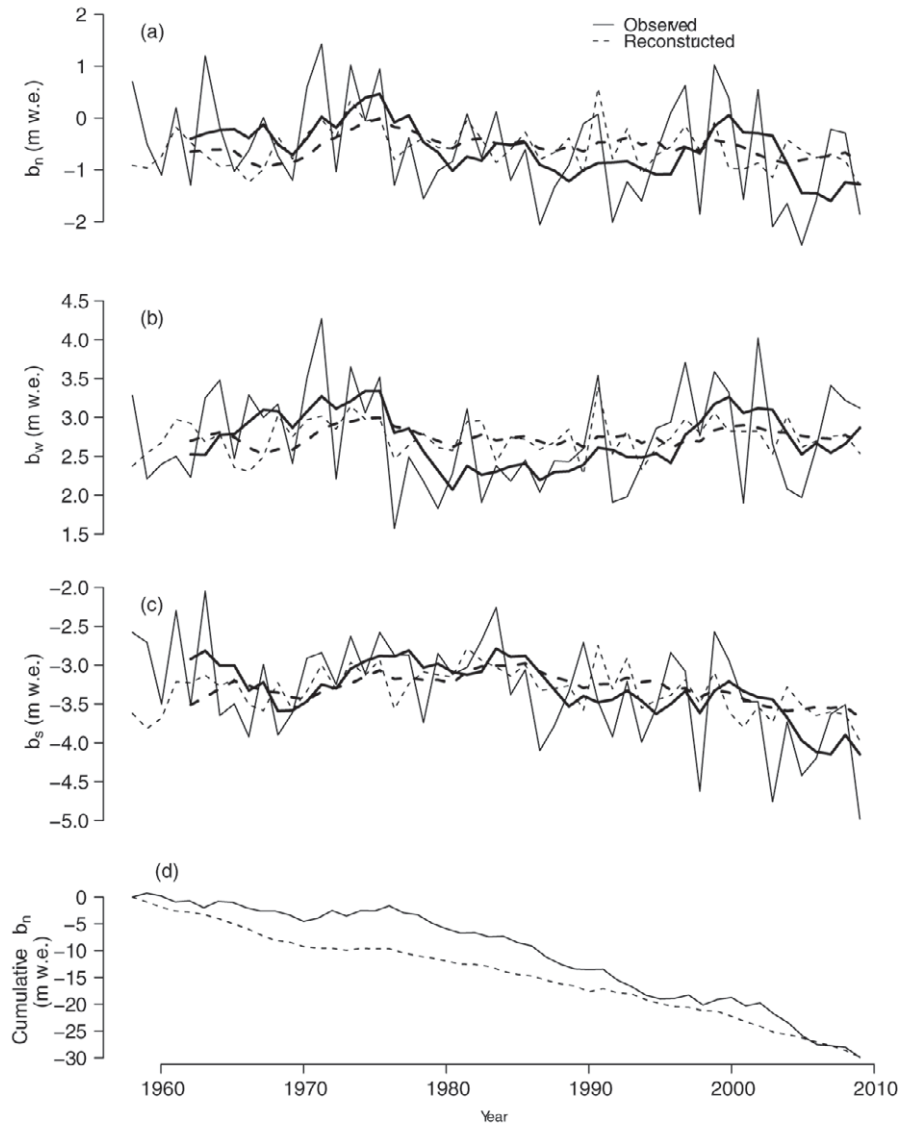
Figure 2. Fitted net (b_n), winter (b_w), and summer (b_s) mass balance (dashed line; meters water equivalent [m w.e.]) plotted against the corresponding observed balance values (solid line) for the measurement period of 1959–2009. Net balance (a) is fitted from residuals PC1, winter balance (b) is from the Minotaur Lake residual chronology, and summer balance (c) used the Hidden Lake residual chronology. A 5-year running mean has been fit to the reconstructed balance (thick dashed line) and the observed balance (thick solid line) to highlight patterns in the shorter measurement period. The bottom graph (d) is a comparison of reconstructed and observed cumulative net mass balance over the measurement period.

observed and reconstructed values emphasizes its conservative response. The observed cumulative balance has more variability, whereas the cumulative reconstruction balance declines steadily. The net, summer, and winter reconstructions have a lower standard deviation than the observed values, but as in any regression, the variance of the fitted values is less than the variance of the observations. In some cases, years of extreme above- or below-average balance are poorly modeled, and the reconstruction model fails to capture the magnitude present in the observed record. In particular, the net reconstruction is unable to capture large positive pulses in the observed record. This slight negative bias is likely because the mean observed record is negative and extreme positive years are too far from the mean for the regression to capture. The 5-year running mean on Figures 2a–c shows that even without capturing every year perfectly, the reconstructed balance follows the patterns of the observed balance over the calibration period.

Reconstructions were standardized to the zero line by adding the mean value of the reconstruction. Standardization was done to create a clearer visualization of above- and below-average mass balance for easier viewing and comparison purposes. A 10-year moving average curve fit to the reconstruction (Figure 3) highlights several extended periods of above-average net mass balance: 1690–1710,
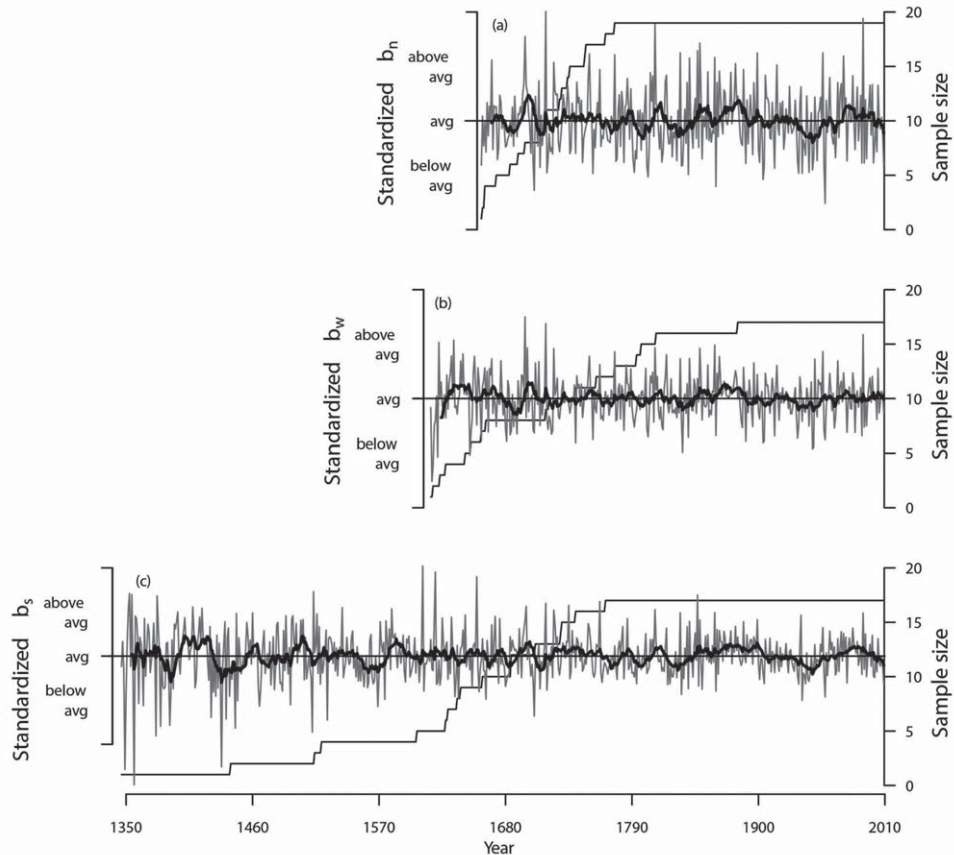
Figure 3. Time series plots of reconstructed net (b_n), winter (b_w), and summer (b_s) mass balance. Net balance (a) is reconstructed from PC1 for 1659–2009, winter balance (b) is reconstructed from the Minotaur Lake residual chronology for the span 1615–2009, and summer balance (c) is reconstructed from the Hidden Lake residual chronology, 1346–2009. The thick black line represents a 10-year moving average. Sample depth is indicated by the thin black line and the right side y-axis, where sample depth for (a) indicates the shortest chronology entered into the PCA. These plots have been standardized by adding in the mean for each individual series in order to show a clearer picture of periods of above- and below-average balance.

1810–1820, 1845–1860, 1865–1890, and 1975–1990. Extended periods of below-average net balance include 1680–1690, 1790–1810, 1820–1840, and 1930–1960. The ML chronology extends from 1615 to 2009 (Figure 3). Prolonged above-average winter balance occurred in 1630–1650, 1660–1680, 1700–1710, 1750–1760, 1810–1820, 1845–1860, 1865–1890, and 1970–1985. Sustained below-average winter balance occurred in 1680–1700, 1720–1730, 1760–1775, 1790–1800, 1830–1845, 1890–1915, 1925–1955. The HL chronology dates from 1346 to 2009 (Figure 3). Although the HL chronology reconstructs 663 years of summer mass balance, as the reconstruction goes further into the past, there are fewer cores represented in the chronology. Because the sample depth of the chronology is low, caution should be used when considering the reliability and statistical structure of the reconstruction in its earliest years. Above-average summer mass balance occurred during 1395–1425, 1495–1510, 1580–1600, 1645–1660, 1690–1705, 1720–1765, 1810–1820, 1845–1905, and 1970–1990. Below-average summer balance persisted during 1425–1455, 1550–1580, 1635–1645, 1680–1690, 1705–1720, 1765–1780, 1790–1805, 1820–1845, and 1920–1955.

Several visual ways to validate the net mass balance reconstruction were also examined. The reconstruction was compared with other reconstructions of glaciers in the PNW, the PDO and ENSO indices, and a net balance created from the sums of the reconstructed summer and winter balances. Periods of above- and below-average net mass balance matched with other reconstructions (Figure 4). The reconstructed net balance followed the negative relationship found between the observed net balance and the PDO and ENSO index values (Figure 5). The summed net balance reconstruction and the net balance reconstructed from PC1 have similar patterns of above- and below-average net balance (Figure 6).

The highest period of net reconstructed mass balance was in the early 1700s and the lowest period was in the 1940s (Figure 7), and rate of change was calculated for several time periods of high to low balance in the reconstruction (Table 6). The fastest rate of change from an above-
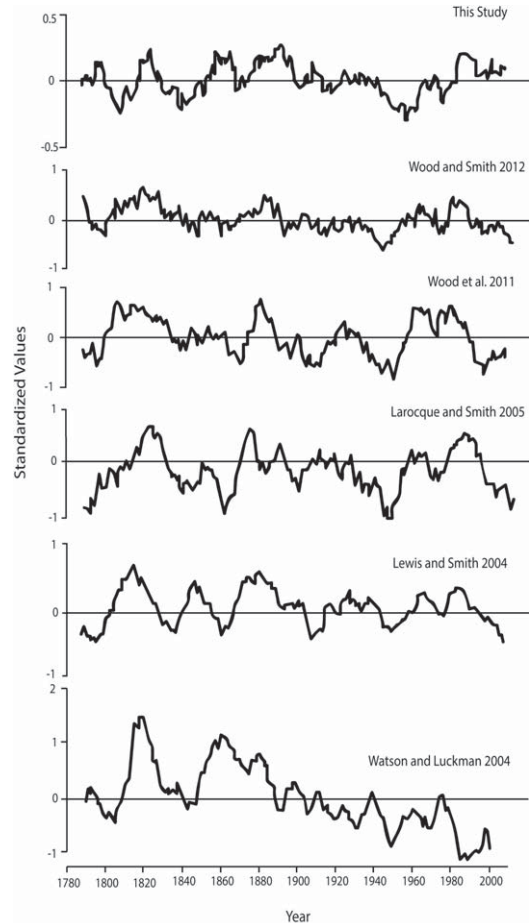
Figure 4. Comparison of the reconstructed net balance created in this study to reconstructed net balance created in similar studies in the Pacific Northwest. Adapted from Wood et al. (2011) and Wood and Smith (2012). The scales and magnitudes of the reconstructions are different and some caution should be taken when interpreting standardized values on the y-axis. The last decade of the South Cascade Glacier reconstruction created in this study is not shown.

average peak to a below-average trough was in the early 1700s, and the slowest rate of change in the reconstructed net balance was in the mid-1970s.

Discussion

Reconstructions of net, summer, and winter balance all have comparable time periods of above-average mass balance (Figure 3). These periods of above-average mass balance are similar to reconstructions of other glaciers in the PNW (Lewis and Smith
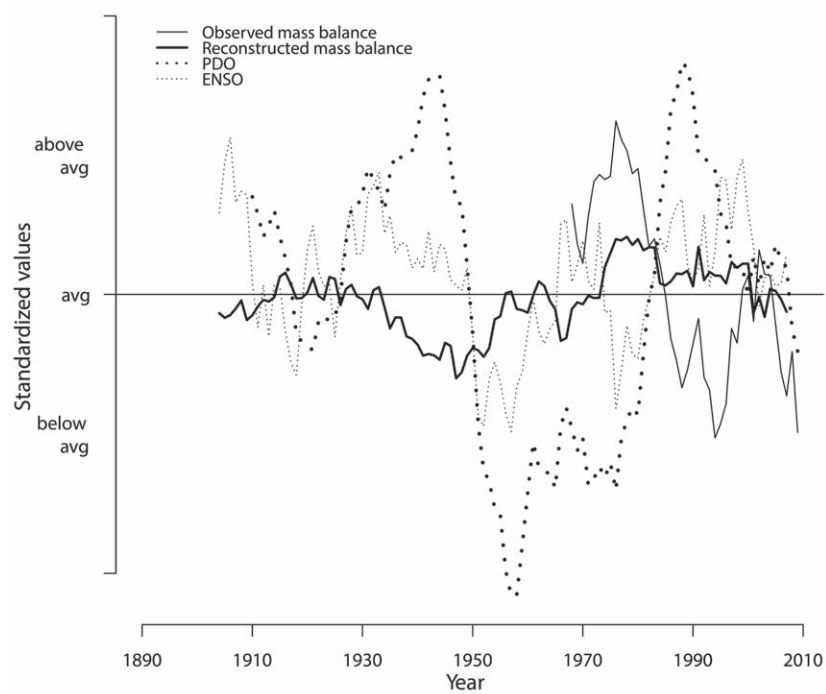
Figure 5. Time series plot of reconstructed net mass balance, observed net mass balance, average winter Pacific Decadal Oscillation (PDO) index values, and average winter Niño 3.4 (ENSO) index. The series are displayed as a 10-year moving average and have all been standardized
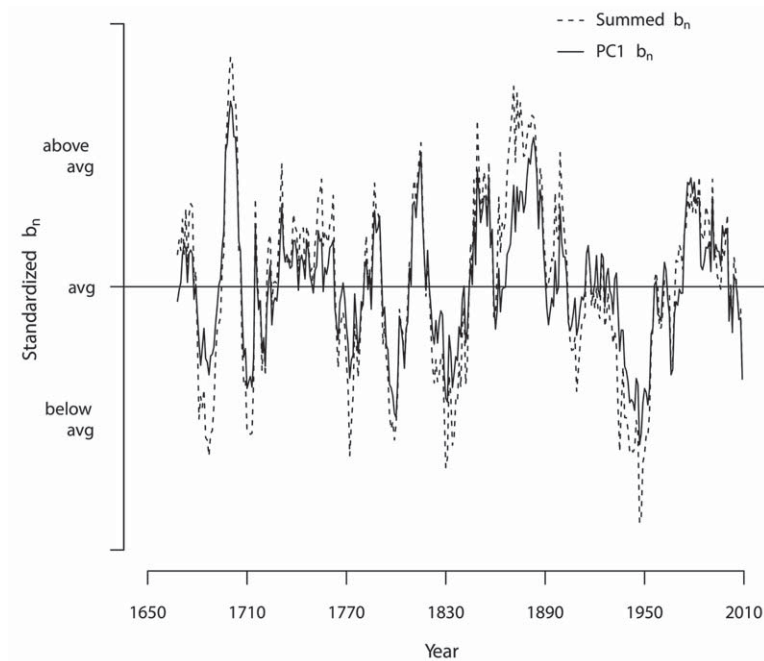
Figure 6. Time series plots of reconstructed net balance. The solid line represents a 10-year moving average of net balance reconstructed from PC1, and the dashed line represents a 10-year moving average of net balance from the sum of the winter and summer mass balances. These series have been standardized.
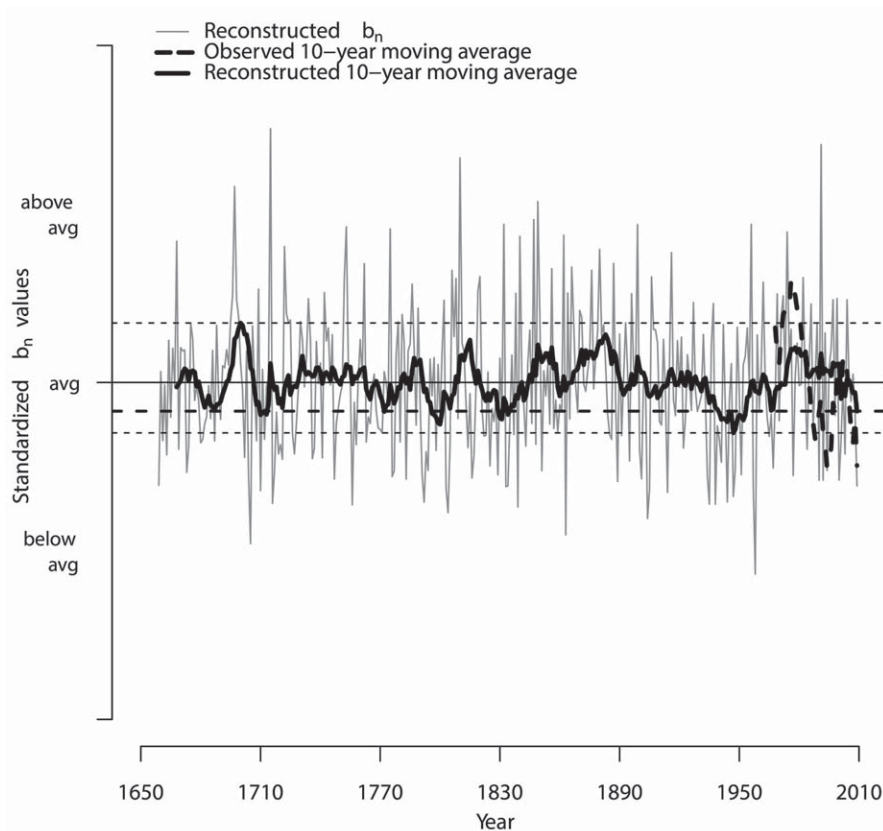
Figure 7. Time series plot of reconstructed and observed net balance (b_n). The thick solid line represents a 10-year moving average of the reconstructed balance, and the thick dashed line is a 10-year moving average for the observed net balance. The thin dashed lines represent the minimum and maximum values of the reconstructed moving average line. The thick long dashed line represents the reconstructed moving average minimum for 2009. All series have been standardized by adding in the mean for each individual series in order to show a clearer picture of periods of above- and below-average balance.

TABLE 6. Rates of change in meters water equivalent per year (m w.e. yr^{-1}) for periods of decreasing net mass balance in the reconstructed and observed record.

Reconstructed net balance			Observed net balance		
Time range	Years	Rate of change (m w.e. yr^{-1})	Time range	Years	Rate of change (m w.e. yr^{-1})
1700–1710	10	-0.055	1976–1988	12	-0.080
1790–1800	10	-0.038	2000–2009	9	-0.062
1815–1831	16	-0.029			
1856–1863	7	-0.036			
1883–1895	9	-0.040			
1925–1947	23	-0.016			
1976–1988	12	-0.010			
2000–2009	9	-0.031			

2004, Watson and Luckman 2004, Larocque and Smith 2005, Wood et al. 2011, Wood and Smith 2012, Malcomb and Wiles 2013) (Figure 4). All reconstructions, including this one, have com-mon above-average periods during 1695–1710, the 1810s, 1820s, 1860–1880, and the 1970s. Similar below-average periods are 1790–1805, 1820–1840, and 1930–1950. The reconstructions

used various tree species from different locations around the PNW, and each reconstruction is for a different glacier or combination of glaciers, yet several periods of sustained above- and below-average mass balance are common, suggesting that glaciers in the PNW are responding to similar climatic forcings. These reconstructions may reflect a regional signal, at least for glaciers with similar topographic features.

Comparison to moraine dates from PNW studies also verifies the regional representation of our SCG reconstruction. Periods of above-average mass balance should coincide with moraine dates. Heikkinen (1984) dated moraines for Coleman Glacier on Mount Baker (about 75 km from SCG) and found dates around 1740, 1820, 1855, late 1880s, 1910, 1920, and the late 1970s. Osborn et al. (2012) also investigated with moraine dates for glaciers on Mount Baker and similarly found that moraines were deposited in the 1820s, 1850s, and 1860s. Both Heikkinen (1984) and Osborn et al. (2012) moraine dates fall after periods of significant above-average reconstructed balance during 1810–1820 and around 1845–1860. Larocque and Smith (2003) investigated moraine dates in the Mt. Waddington area of the Coast Mountains and found that glaciers deposited moraines in 1770–1785, 1820–1840, 1870–1900, 1915–1930, and the mid-1940s. Koch et al. (2007) dated moraines of glaciers in Garibaldi Provincial Park, also in the southern Coast Mountains, and concluded that the most extensive moraine-building episode occurred during 1690–1720. Other moraine dates found by Koch et al. (2007) include the 1820s, 1870s, and 1900s. Dates by Koch et al. (2007) and Larocque and Smith (2003) for the Coast Mountains correspond to several periods of above-average glacier mass balance, especially 1690–1710, 1810–1820, and 1845–1860. The majority of these moraine dates in the PNW occurred during or just after periods of above-average reconstructed SCG mass balance.

A few shorter-term reconstructions of SCG balance have been created. Tangborn (1980) used monthly temperature and precipitation records to model SCG mass balance for 1884–1974. Rasmussen (2009) reconstructed SCG balance for 1935–1958 from daily precipitation and temperature records, and he also adjusted the observations (1959–2006) to constant-topography values. These net balance reconstructions had similar below-average periods (1940s) and above-average periods (1970s) as the reconstruction in this study, although there are disagreements, such as during 1910–1930 when Tangborn (1980) reconstructs below-average mass balance and our study reconstructs mostly average net balance. The reconstruction in this study fails to capture the magnitude in these reconstructions, but it does follow the patterns of the peaks and troughs. The differences between these reconstructions may have been caused by the variables used in creating the model, such as temperature and precipitation records or the use of PCA.

In their extensive study of PNW glaciers, Larocque and Smith (2005) reconstructed SCG winter balance for 1835–1999. They found periods of above-average winter balance in 1860–1890, 1895–1900, 1910–1920, 1950–1965, and 1975–1985. The winter balance reconstructed in this study was above average during the similar periods of 1865–1890 and 1970–1985. Below-average balance was found in both reconstructions during the 1910s and 1940s. Although there is agreement between these two reconstructions, there are discrepancies such as the above-average winter balance Larocque and Smith (2005) reconstructed for 1910–1920. During this time period our reconstruction is mainly neutral, with small fluctuations between above- and below-average mass balance. The discrepancies could be caused by reconstruction methods and location of sampling sites for the tree chronologies. This study used sites near SCG, and Larocque and Smith (2005) used cores from farther away that may have had different local conditions.

Malcomb and Wiles (2013) also completed an extensive study of PNW glacier mass balance, in which they reconstructed annual balance at SCG for 1580–1992. Similar to our study, periods of above-average mass balance were found in the early and mid-1700s, around 1810, the late 1800s, and the 1970s, and below-average balance occurred during the late 1700s, around 1820–1840, and

1930–1950. Again, there are both agreements and disagreements between our reconstruction and Malcolmb and Wiles (2013), which could be the result of differing methodologies like the location of sites and shorter calibration period (1959–1992).

There is general agreement in mass balance patterns between the reconstruction in this study and those created in other studies in the PNW. The similarity in patterns is emphasized, because the reconstructions have different units and scales, which are sensitive to the data processes, and it is not appropriate to compare the absolute changes and the magnitude of responses. For example, the net balance reconstruction in this study is created from PCA, where the original growth time series has been transformed and rotated into a linear combination of the growth indices, which complicates comparisons with other reconstructions. Therefore, comparisons of reconstructions are more appropriate for overall similarity in mass balance patterns rather than changes in magnitude and scale of the reconstructions.

The PDO and ENSO index values had significant negative correlations with mass balance and positive correlations with tree growth (Table 3, 4). Warm phases of PDO and ENSO correspond to lower mass balance and higher tree radial growth, and increased balance and decreased growth occur during cool phases. The reconstructed net balance matches the negative relationship found between the observed and index values (Figure 5). Correlations with the PDO index were expected, as shown in other PNW glacier studies (Hodge et al. 1998, Bitz and Battisti 1999, Moore and Demuth 2001, Lewis and Smith 2004, Pederson et al. 2004, Larocque and Smith 2005, Watson et al. 2006, Pelto 2008, Malcomb and Wiles 2013). However, this study also found that the ENSO index is significantly correlated with mass balance at SCG, despite disagreement in the literature (Hodge et al. 1998, Bitz and Battisti 1999, Moore and Demuth 2001 [weak correlation with ENSO], Larocque and Smith 2005, Watson et al. 2006, Pelto 2008, Wood et al. 2011 [correlation with ENSO]). Glacier studies in the PNW have shown that PNA primarily influences mass balance (Hodge et al.

1998, Bitz and Battisti 1999, Wood et al. 2011). Although significant correlations between mass balance and the PNA index were found in this study, the results suggest that ENSO has a stronger relationship with SCG balance. The wide variety of correlation results for ocean-atmosphere oscillation indices in studies around the PNW indicates a complicated relationship between glacier mass balance and these oscillations.

Summing the winter and summer reconstructions can create a net balance reconstruction. The reconstruction from summing the winter and summer fitted values was compared to the net reconstruction from the PC1 chronology (Figure 6). The summed and PC1 reconstructions are nearly identical, with similar patterns of above- and below-average net balance, although the summed reconstruction does have more variability. This comparison confirms the suitability of both approaches for reconstructing net balance and improves confidence in the PC1 reconstruction patterns.

Based on the moving average of the reconstructed values, the highest period of net mass balance occurred around 1700 and the lowest period occurred around 1940 (Figure 7). This below-average period in the 1940s occurred after an extended time of low precipitation in the 1930s. Over the measurement record (1959–2009) the reconstruction was lowest in 2009, yet this low balance and subsequent increase have occurred before (Figure 7). The observed record shows much lower balance for 2009, and although the reconstructed values are similar to the observed record, the reconstructed magnitude and variability are conservative. The reconstruction of net balance also shows slight above-average mass balance for 1980–1995, but the observations during most of this time are below average. This time period also disagrees with prior reconstructions in the PNW, which are below average around 1990 (Figure 4). The year 1991 was unusually high in the time series of reconstructed values. This was a marker year in our tree-ring growth chronologies, because it was consistently small and easy to identify. This indicates a poor growth year for mountain hemlock, yet it was not reflected in SCG mass balance. A

short-term climatic event, such as a late freeze, may have affected tree growth, but would not have influenced mass balance. It has been previously shown that extreme climatic events can affect the relationship and reconstruction potential of tree growth and mass balance (Leonelli et al. 2008, Leonelli et al. 2011). Because 1991 is predicted to be high, the reconstructed 10-year running mean is overestimated and shows above-average mass balance when the record and other PNW reconstructions do not. This is the only obvious divergent response from other reconstructions, and in general, the patterns of above- and below-average reconstructed mass balance are consistent in the PNW. After this unusual period in the 1990s, both the reconstructed and observed values concur about a recent decline.

The recent decrease in mass balance can also be assessed by examining the rate of change between high and low peaks of mass balance. Rate of change was calculated for several time periods in which mass balance switched from above-average to below-average in the 10-year moving average of the reconstruction (Table 6). The 1940s were the period with the lowest balance in the reconstructed record, although the decline was gradual. The recent decline in the reconstruction, 2000–2009, has the fastest rate in over a century. The only comparable rate of decrease to the observed values was around 1700, where the reconstruction shows the largest peak in net mass balance (Figure 7). As discussed earlier, the reconstruction does have a lower variability than the observed record and a slight bias towards negative values caused by the use of regression. The limitations of the reconstruction affect the way we interpret results. For example the reconstruction fails to accurately represent extreme highs and lows in the observed record (normal for regression), causing the rate of change between high and low peak periods to be underestimated.

Annual mean temperature in nearby Stehekin, Washington, has increased by 0.12 °C per decade during 1895–2010 (Office of the Washington State Climatologist 2014). Mean temperature during 1895–1905 was 7.8 ºC, increasing to 9.0 °C by 2000–2010, and temperature in the 21st century is projected to increase, on average, 0.3 °C per decade (Mote and Salathé 2010). Because of the negative relationship between temperature and mass balance, the increase in temperature is expected to cause a decrease in mass balance. For 2000–2009, SCG net mass balance averaged a decrease of 1.08 meters water equivalent (m w.e.) (calculated from the observed record), while annual divisional temperatures increased 0.06 °C. If temperatures increase by 0.3 °C per decade, SCG could experience decreases of approximately 5.40 m w.e per decade. This projection assumes that (1) the established relationship is between temperature and mass balance, not glacial extent (such as advance/retreat), (2) the relationship is assumed to be roughly linear, and (3) temperature is the primary variable affecting balance. The projection does not account for the effect winter precipitation and snowpack have on SCG mass balance or the role cool-season precipitation will play in moderating future mass loss.

Recent glacier recession is primarily influenced by warming spring and summer temperatures, although variability in winter precipitation is still an important driving factor for glacier behavior (McCabe et al. 2000, Pederson et al. 2004, Rasmussen and Conway 2004, Watson and Luckman 2004, Pelto 2006). Spring snow-covered area, snowpack, and SWE are decreasing in the PNW in accordance with rising temperatures over the last 30–40 years (Mote et al. 2005, McCabe and Wolock 2010, Pederson et al. 2011). With less precipitation falling as snow, there will be less accumulation to prevent additional mass loss. Recent warming has also likely led to a weakening correlation between mass balance and PDO over the past two decades, and these changes could overwhelm the current observed negative relationship (Josberger et al. 2009). This inference is supported by the winter PDO index being relatively stable around zero since 2000 before declining again, yet mass balance has continued to decrease (Figure 5). It appears that the recent decrease could be attributed to a period of warmer temperature, rather than the influence of climatic modes of variability.

There are around 300 glaciers covering over 100 km² and yielding millions of cubic meters of runoff annually in just the North Cascade National Park Complex (Granshaw and Fountain 2006). Within the last 20–30 years, PNW glacier-fed streams have experienced a decline in late-summer flow, and with continued glacier retreat, this decline is expected to intensify (Moore and Demuth 2001, Stahl and Moore 2006, Nolin et al. 2010, Pelto 2011), causing higher stream temperature, higher sedimentation, and lower water quality (Moore et al. 2009). South Cascade Glacier has recovered from low mass balance periods like the one experienced in the last decade, but the rate of this decline is faster than it has been in a century. If this trend continues and increases in magnitude, the PNW will experience significant changes in glacier-influenced water resources.

Literature Cited

Bidlake, W. R., E. G. Josberger, and M. E. Savoca. 2010. Modeled and measured glacier change and related glaciological, hydrological, and meteorological conditions at South Cascade Glacier, Washington, balance and water years 2006 and 2007. U.S. Geological Survey Scientific Investigations Report 2010-5143.

Bitz, C. M., and D. S. Battisti. 1999. Interannual to decadal variability in climate and the glacier mass balance in Washington, western Canada, and Alaska. Journal of Climate 12:3181-3196.

Burbank, D. W. 1982. Correlations of climate, mass balances, and glacial fluctuations at Mount Rainier, Washington, USA, since 1850. Arctic and Alpine Research 14:137-148.

Cook, E. R., and R. L. Holmes. 1996. Guide for computer program ARSTAN. *In* H. D. Grissino-Mayer, R. L. Holmes, and H. C. Fritts (editors), The international tree-ring data bank program library version 2.0 user's manual. University of Arizona, Tucson. Pp. 75-87.

Dyurgerov, M. B., and M. F. Meier. 1999. Analysis of winter and summer glacier mass balances. Geografiska Annaler 81A:541-554.

Fountain, A. G., M. J. Hoffman, F. Granshaw, and J. Riedel. 2009. The 'benchmark glacier' concept—does it work? Lessons from the North Cascade Range, USA. Annals of Glaciology 50:163-168.

Fritts, H. C. 1976. Tree rings and climate. Academic Press, London.

Gedalof, Z., and D. J. Smith. 2001. Dendroclimatic response of mountain hemlock (*Tsuga mertensiana*) in Pacific North America. Canadian Journal of Forest Research 31:322-332.

Granshaw, F. D., and A. G. Fountain. 2006. Glacier change (1958-1998) in the North Cascades National Park Complex, Washington, USA. Journal of Glaciology 52:251-256.

Heikkinen, O. 1984. Dendrochronological evidence of variations of Coleman Glacier, Mount Baker, Washington, USA. Arctic and Alpine Research 16:53-64.

Hodge, S. M., D. C. Trabant, R. M. Krimmel, T. A. Heinrichs, R. S. March, and E. G. Josberger. 1998. Climate variations and changes in mass of three glaciers in western North America. Journal of Climate 11:2161-2179.

Holmes, R. L. 1983. Computer assisted quality control in tree-ring dating and measurement. Tree-Ring Bulletin 43:69-78.

Josberger, E. G., W. R. Bidlake, R. S. March, and S. O'Neel. 2009. Fifty-year record of glacier change reveals shifting climate in the Pacific Northwest and Alaska, USA. U.S. Geological Survey Fact Sheet 2009-3046.

Koch, J., J. J. Clague, and G. D. Osborn. 2007. Glacier fluctuations during the past millennium in Garibaldi Provincial Park, southern Coast Mountains, British Columbia. Canadian Journal of Earth Sciences 44:1215-1233.

Koch, J., B. Menounos, and J. J. Clague. 2009. Glacier change in Garibaldi Provincial Park, southern Coast

Mountains, British Columbia, since the Little Ice Age. Global and Planetary Change 66:161-178.

Larocque, S. J., and D. J. Smith. 2003. Little Ice Age glacial activity in the Mt. Waddington area, British Columbia Coast Mountains, Canada. Canadian Journal of Earth Sciences 40:1413-1436.

Larocque, S. J., and D. J. Smith. 2005. 'Little Ice Age' proxy glacier mass balance records reconstructed from tree rings in the Mt Waddington area, British Columbia Coast Mountains, Canada. The Holocene 15:748-757.

Leonelli, G., M. Pelfini, and P. Cherubini. 2008. Exploring the potential of tree-ring chronologies from the Trafoi Valley (Central Italian Alps) to reconstruct glacier mass balance. Boreas 37:169-178.

Leonelli, G., M. Pelfini, R. D'Arrigo, W. Haeberli, and P. Cherubini. 2011. Non-stationary responses of tree-ring chronologies and glacier mass balance to climate in the European Alps. Arctic, Antarctic, and Alpine Research 43:56-65.

Lewis, D., and D. Smith. 2004. Dendrochronological mass balance reconstruction, Strathcona Provincial Park, Vancouver Island, British Columbia, Canada. Arctic Antarctic and Alpine Research 36:598-606.

Malcomb, N. L., and G. C. Wiles. 2013. Tree-ring-based reconstructions of North American glacier mass balance through the Little Ice Age—Contemporary warming transition. Quaternary Research 79:123-137.

Mantua, N. J., S. R. Hare, Y. Zhang, J. M. Wallace, and R. C. Francis. 1997. A Pacific interdecadal climate oscillation with impacts on salmon production. Bulletin of the American Meteorological Society 78:1069-1079.

McCabe, G. J., and A. G. Fountain. 1995. Relations between atmospheric circulation and mass balance at South Cascade Glacier, Washington, USA. Arctic and Alpine Research 27:226-233.

McCabe, G. J., A. G. Fountain, and M. Dyurgerov. 2000. Variability in winter mass balance of Northern Hemisphere glaciers and relations with atmospheric circulation. Arctic, Antarctic, and Alpine Research 32:64-72.

McCabe, G. J., and D. M. Wolock. 2010. Long-term variability in Northern Hemisphere snow cover and associations with warmer winters. Climatic Change 99:141-153.

Meier, M. F., M. B. Dyurgerov, and G. J. McCabe. 2003. The health of glaciers: Recent changes in glacier regime. Climatic Change 59:123-135.

Moore, R. D., and M. N. Demuth. 2001. Mass balance and streamflow variability at Place Glacier, Canada, in relation to recent climate fluctuations. Hydrological Processes 15:3473-3486.

Moore, R. D., S. W. Fleming, B. Menounos, R. Wheate, A. Fountain, K. Stahl, K. Holm, and M. Jakob.

2009. Glacier change in western North America: influences on hydrology, geomorphic hazards and water quality. Hydrological Processes 23:42-61.

Mote, P. W., A. F. Hamlet, M. P. Clark, and D. P. Lettenmaier. 2005. Declining mountain snowpack in western North America. Bulletin of the American Meteorological Society 86:39-49.

Mote, P. W., and E. P. Salathé. 2010. Future climate in the Pacific Northwest. Climatic Change 102:29-50.

NCAR (National Center for Atmospheric Research). 2008. Niño 3.4 Index. Climate and Global Dynamics, Climate Analysis Section, Boulder, CO. Available online at http://www.cgd.ucar.edu/cas/catalog/climind/TNI_N34/index.html#Sec5 (accessed September 2011).

NOAA (National Oceanic and Atmospheric Administration). 2012. Antarctic Oscillation, Arctic Oscillation, North Atlantic Oscillation, Pacific-North American Pattern. National Weather Service, NOAA Center for Weather and Climate Prediction, Climate Prediction Center, College Park, MD. Available online at http://www.cpc.ncep.noaa.gov/products/precip/CWlink/daily_ao_index/teleconnections.shtml (accessed September 2011).

Nolin, A. W., J. Phillippe, A. Jefferson, and S. L. Lewis. 2010. Present-day and future contributions of glacier runoff to summertime flows in a Pacific Northwest watershed: implications for water resources. Water Resources Research 46:W12509, doi:10.1029/2009WR008968.

Office of the Washington State Climatologist. 2014. N.W. Temperature, Precipitation, and SWE Trend Analysis. University of Washington, Seattle, WA. Available online at http://www.climate.washington.edu/trendanalysis/ (accessed online March 2012).

Osborn, G. D., Menounos, B. P., Ryane, C., Riedel J., Clague, J. J., Koch, J., Clark, D., Scott, K., and P. T. Davis. 2012. Latest Pleistocene and Holocene glacier fluctuations on Mount Baker, Washington. Quaternary Science Reviews, 49:33-51.

Pederson, G. T., D. B. Fagre, S. T. Gray, and L. J. Graumlich. 2004. Decadal-scale climate drivers for glacial dynamics in Glacier National Park, Montana, USA. Geophysical Research Letters 31.

Pederson, G. T., S. T. Gray, C. A. Woodhouse, J. L. Betancourt, D. B. Fagre, J. S. Littell, E. Watson, B. H. Luckman, and L. J. Graumlich. 2011. The unusual nature of recent snowpack declines in the North American Cordillera. Science 333:332-335.

Pelto, M. S. 2006. The current disequilibrium of North Cascade glaciers. Hydrological Processes 20:769-779.

Pelto, M. S. 2008. Glacier annual balance measurement, forecasting and climate correlations, North Cascades, Washington 1984-2006. Cryosphere 2:13-21.

Pelto, M.S. 2011. Skykomish River, Washington: impact of ongoing glacier retreat on streamflow. Hydrological Processes 25:3356-3363.

Peterson, D. W., and D. L. Peterson. 2001. Mountain hemlock growth responds to climatic variability at annual and decadal time scales. Ecology 82:3330-3345.

R Development Core Team, 2010. R: A language and environment for statistical computing. Vienna, Austria: R Foundation for Statistical Computing.

Rasmussen, L. A. 2009. South Cascade Glacier mass balance, 1935-2006. Annals of Glaciology 50:215-220.

Rasmussen, L. A., and H. Conway. 2004. Climate and glacier variability in western North America. Journal of Climate 17:1804-1815.

Stahl, K., and R. D. Moore. 2006. Influence of watershed glacier coverage on summer streamflow in British Columbia, Canada. Water Resources Research 42:W06201, doi:10.1029/2006WR005022.

Stokes, M. A., and T. L. Smiley. 1968. An Introduction to Tree-Ring Dating. University of Arizona Press, Tucson.

Tangborn, W. 1980. Two models for estimating climate-glacier relationships in the North Cascades, Washington, USA. Journal of Glaciology 25:3-21.

University of Washington. 2014. Pacific Decadal Oscillation Index Monthly Values. Joint Institute for the Study of Atmosphere and Ocean, Seattle, WA. Available online at http://margaret.atmos.washington.edu/pdo/PDO.latest (accessed September 2011).

Walters, R. A., and M. F. Meier. 1989. Variability of glacier mass balances in western North America. *In* D. H. Peterson (editor), Aspects of Climate Variability in the Pacific and Western Americas, Geophysical Monograph Series 55. American Geophysical Union, Washington, DC. Pp. 365-374.

Watson, E., and Luckman, B. H., 2004. Tree-ring-based mass-balance estimates for the past 300 years at Peyto Glacier, Alberta, Canada. Quaternary Research 62:9-18.

Watson, E., B. H. Luckman, and B. Yu. 2006. Long-term relationships between reconstructed seasonal mass balance at Peyto Glacier, Canada, and Pacific sea surface temperatures. Holocene 16:783-790.

Wood, L. J., D. J. Smith, and M. N. Demuth. 2011. Extending the Place Glacier mass-balance record to AD 1585, using tree rings and wood density. Quaternary Research 76:305-313.

Wood, L. J., and D. J. Smith. 2012. Climate and glacier mass balance trends from AD 1780 to present in the Columbia Mountains, British Columbia, Canada. The Holocene 23:739-748.